Locally Recurrent Prostate Cancer after External Beam Radiation Therapy: Diagnostic Performance of 1.5-T Endorectal MR Imaging and MR Spectroscopic Imaging for Detection[1]

Antonio C. Westphalen, MD
Fergus V. Coakley, MD
Mack Roach III, MD
Charles E. McCulloch, PhD
John Kurhanewicz, PhD

Purpose: To determine if performing magnetic resonance (MR) spectroscopic imaging, compared with performing T2-weighted MR imaging alone, improves the detection of locally recurrent prostate cancer after definitive external beam radiation therapy.

Materials and Methods: This retrospective single-institution study was approved by the committee on human research, with a waiver of informed consent, and was compliant with HIPAA requirements. Sixty-four men who underwent endorectal MR imaging, MR spectroscopic imaging, and transrectal ultrasonographically guided biopsy for suspected local recurrence of prostate cancer after definitive external beam radiation therapy were retrospectively identified. Thirty-three patients had also received androgen therapy. Recurrent cancer was determined to be present or absent in the left and right sides of the prostate at T2-weighted MR imaging and MR spectroscopic imaging by a radiologist and a spectroscopist, respectively. Area under the receiver operating characteristic curve (A_z) was calculated for T2-weighted MR imaging alone and combined T2-weighted MR imaging and MR spectroscopic imaging by using generalized estimating equations and by using biopsy results as the reference standard.

Results: Recurrent prostate cancer was identified at biopsy in 37 (58%) of the 64 men. Recurrence was unilateral in 28 patients and bilateral in nine (total of 46 affected prostate sides). A_z analysis revealed that use of combined T2-weighted MR imaging and MR spectroscopic imaging (A_z = 0.79), as compared with T2-weighted MR imaging alone (A_z = 0.67), significantly improved the detection of local recurrence (P = .001).

Conclusion: The addition of MR spectroscopic imaging to T2-weighted MR imaging significantly improves the diagnostic accuracy of endorectal MR imaging in the detection of locally recurrent prostate cancer after definitive external beam radiation therapy.

[1] From the Departments of Radiology and Biomedical Imaging (A.C.W., F.V.C., J.K.), Radiation Oncology (M.R.), and Epidemiology and Biostatistics (C.E.M.), University of California San Francisco, 505 Parnassus Ave, Box 0628, M-372, San Francisco, CA 94143-0628. Received December 20, 2009; revision requested February 2, 2010; revision received February 10; final version accepted February 24. A.C.W. supported by RSNA Research and Education Foundation 2006–07 Research Fellow grant FEL0602 and RSNA Research and Education Foundation 2007–2009 Research Scholar grant RSCH0709. **Address correspondence to** A.C.W. (e-mail: *antonio.westphalen@radiology.ucsf.edu*).

Approximately 200 000 American men received a diagnosis of prostate cancer in 2009 (1), and up to 25% of them chose external beam radiation therapy as their definitive treatment (2–4). Patients treated with external beam radiation therapy are followed up with serial measurements of their serum prostatic-specific antigen (PSA) levels. Biochemical failure (increasing PSA level after a nadir level) is seen in approximately 50% of patients after 5 years, depending on the pretreatment risk factors. Once biochemical failure occurs, further investigation is initiated to determine the presence or absence of recurrent disease, which can be local (25%–30% of cases), systemic (20%–25% of cases), or both (45%–55% of cases) (5–14). The detection or exclusion of local recurrence influences the therapeutic choices for patients with postradiation biochemical failure, which include surveillance, systemic hormonal therapy, and salvage prostatectomy. Transrectal ultrasonography (US)-guided sextant biopsy is the current reference standard for the detection of local recurrence of prostate cancer in patients with biochemical failure after external beam radiation therapy, but it is invasive and may fail to depict some tumors because only a small fraction of the gland is sampled. An accurate noninvasive alternative that enabled assessment of the entire gland would be preferable.

In recent years, endorectal magnetic resonance (MR) imaging, particularly that performed by using T2-weighted sequences, has emerged as an exciting modality for the local detection and characterization of prostate cancer. Standard T2-weighted MR imaging of the irradiated prostate may be limited by the posttreatment loss of zonal anatomy and diffuse low T2 signal, which hinder tumor detection (15–18). As a result, MR spectroscopic imaging, a technique that enables the detection of abnormal metabolism rather than abnormal anatomy, has been investigated in this setting and yielded promising results in earlier studies (15,16,19). These studies have been small and did not fully address the incremental value of MR spectroscopic imaging compared with T2-weighted MR imaging alone. Accordingly, we undertook this study to determine if the addition of MR spectroscopic imaging, as compared with T2-weighted MR imaging alone, improves the detection of locally recurrent prostate cancer after definitive external beam radiation therapy.

Advance in Knowledge

- The addition of MR spectroscopic imaging to T2-weighted MR imaging significantly improves the detection of locally recurrent prostate cancer after definitive external beam radiation therapy; in the current study, the area under the receiver operating characteristic curve increased from a fair value (0.67) to a good value (0.79).

Implication for Patient Care

- The information obtained with combined T2-weighted MR imaging and MR spectroscopic imaging may assist clinicians in advising patients about subsequent clinical evaluation and selecting those patients for whom targeted prostate-side biopsy is appropriate for confirming disease.

Materials and Methods

Patient Population

This retrospective single-institution study was approved by our committee on human research, with the requirement for informed consent waived, and was compliant with the requirements of the Health Insurance Portability and Accountability Act. We retrospectively searched our medical and radiologic databases to identify all patients who met the following inclusion criteria: biopsy-proven prostate cancer and primary definitive treatment with external beam radiation therapy (with or without associated neoadjuvant or adjuvant androgen deprivation therapy); posttreatment 1.5-T endorectal MR imaging and MR spectroscopic imaging of the prostate performed between February 1999 and February 2008 because of postradiation biochemical failure, based on the then prevailing 1996 American Society for Therapeutic Radiology and Oncology definition (20) (Such referrals represent routine clinical practice at our institution.); posttreatment transrectal US-guided biopsy performed within 180 days before or after MR imaging; and no postradiation salvage treatment administered before MR imaging or biopsy.

Sixty-four patients fulfilled the described criteria. There were no exclusion criteria. Fifty-nine of these men had been included in a prior study involving investigation of the use of T2-weighted MR imaging alone for the detection of recurrent prostate cancer after external beam radiation therapy (18). One author (A.C.W., 5 years of expertise in genitourinary imaging) reviewed all medical and clinical records to collect all available pretreatment, posttreatment, and histopathologic data.

MR Imaging and Spectroscopic Imaging Technique

MR imaging examinations were performed by using a 1.5-T whole-body MR unit (Signa; GE Medical Systems, Milwaukee, Wis). Patients were imaged

Published online before print
10.1148/radiol.10092314

Radiology 2010; 256:485–492

Abbreviations:
A_z = area under receiver operating characteristic curve
PSA = prostatic-specific antigen

Author contributions:
Guarantors of integrity of entire study, A.C.W., F.V.C.; study concepts/study design or data acquisition or data analysis/interpretation, all authors; manuscript drafting or manuscript revision for important intellectual content, all authors; manuscript final version approval, all authors; literature research, A.C.W.; clinical studies, M.R., J.K.; statistical analysis, A.C.W., C.E.M.; and manuscript editing, A.C.W., F.V.C., M.R., J.K.

Funding:
This research was supported by the National Institutes of Health (grants KL2 RR024130, R01CA079980).

Authors stated no financial relationship to disclose.

by using the body coil for excitation and a pelvic phased-array coil (GE Medical Systems) in combination with a commercially available balloon-covered expandable endorectal coil (Medrad, Pittsburgh, Pa) for signal reception. After a localizer image was obtained, T1-weighted spin-echo MR images (766/8 [repetition time msec/echo time msec], section thickness, 5 mm; intersection gap, 1.5 mm; field of view, 24 cm; matrix, 256 × 192; anteroposterior frequency encoding; one signal acquired) of the pelvis were obtained. The MR sequences also included thin-section high nominal spatial resolution axial and coronal T2-weighted fast spin-echo images of the prostate and seminal vesicles obtained with the following parameters: 5000/96, echo train length of 16, section thickness of 3 mm, intersection gap of 0 mm, field of view of 14 cm, matrix of 256 × 192, anteroposterior frequency encoding (to prevent obscuring of prostate by endorectal coil motion artifact), and three signals acquired.

After review of the axial T2-weighted images, an MR spectroscopic imaging volume that would maximize coverage of the prostate while minimizing the inclusion of periprostatic fat and rectal air was selected by an experienced spectroscopist (J.K., 18 years of experience). Three-dimensional MR spectroscopic imaging data were acquired by using a water- and lipid-suppressed double–spin-echo point-resolved spectroscopy sequence with spectral-spatial pulses for the two 180° excitation pulses, which was optimized for the quantitative detection of choline, creatine, polyamines, and citrate (21,22). Outer-voxel saturation pulses were used to further sharpen the volume selection and conform the selected volume to the shape of the prostate (to eliminate susceptibility artifact from periprostatic fat and rectal air) (23). Data sets were acquired with 16 × 8 × 8 phase-encoded spectral arrays (1024 voxels with a spatial resolution of 0.24–0.34 cm^3), 1000/130, and a 17-minute acquisition time. Three-dimensional MR spectroscopic imaging data were processed offline at an UltraSparc workstation (Sun Microsystems, Mountain View, Calif) by using in-house software that was previously developed specifically for three-dimensional MR spectroscopic imaging examinations. Integrated peak area values for choline, creatine, and citrate, and peak choline-to-creatine and choline plus creatine–to-citrate area ratios were automatically calculated for each voxel. MR spectroscopic imaging data (ie, spectra and associated metabolic ratios) were overlaid on the corresponding axial T2-weighted MR images (Fig 1).

MR Image Interpretation

A single experienced radiologist (F.V.C., 13 years of expertise in genitourinary imaging) reviewed all MR images on a picture archiving and communication system workstation (Impax; Agfa, Mortsel, Belgium) and judged recurrent cancer to be present or absent in the left and right sides of the prostate. The presence of tumor was based on expert judgment rather than strict objective criteria, but in general, tumor was considered to be present if a masslike nodule was seen in the prostate or a crescentic subcapsular focus of low T2 signal intensity was seen in the peripheral zone (24). An experienced spectroscopist (J.K., 18 years of experience) independently reviewed all MR spectroscopic data at the UltraSparc workstation and judged recurrent cancer to be present or absent in the left and right sides of the prostate. The spectroscopist also had access to T2-weighted MR images so that potentially confounding partial volume effects could be incorporated into the final expert spectroscopic evaluation. Muscle, for example, is known

Figure 1

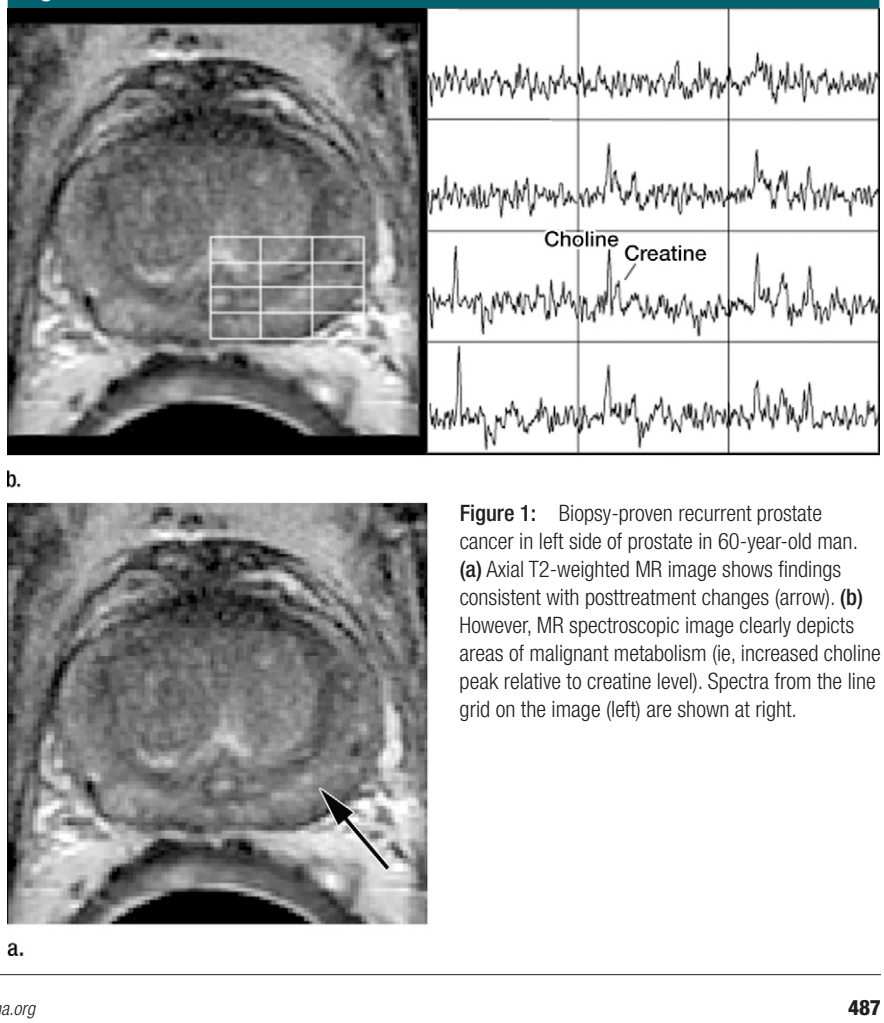

Figure 1: Biopsy-proven recurrent prostate cancer in left side of prostate in 60-year-old man. **(a)** Axial T2-weighted MR image shows findings consistent with posttreatment changes (arrow). **(b)** However, MR spectroscopic image clearly depicts areas of malignant metabolism (ie, increased choline peak relative to creatine level). Spectra from the line grid on the image (left) are shown at right.

to contain choline (25); therefore, voxels that included both prostatic and muscular tissue had elevated choline peaks owing to partial volume averaging effects—not prostate cancer. The spectroscopist used T2-weighted images to identify such voxels and exclude them from the analysis. The interpretation of MR images, however, was based solely on the final metabolic peak ratios and the number of abnormal voxels.

An MR spectroscopic imaging finding was considered to be positive if three or more contiguous ipsilateral voxels with elevated choline levels and no citrate were detected. If creatine was detectable, elevated choline level was defined as a choline-to-creatine ratio greater than 1.5:1. If creatine was absent, elevated choline level was defined as a choline peak area–to-noise ratio greater than 5:1 (26). The readers independently reviewed the data during separate sessions, and no consensus meeting was held to address discrepancies between them. Both readers knew that the patients previously had undergone external beam radiation therapy for prostate cancer and were referred for biochemical failure, but they were blinded to all other clinical and histologic information.

Statistical Analyses

Prostate side was used as the unit of analysis in this study. Our decision to localize MR spectroscopic abnormalities to the side of the prostate instead of to the sextant was based on previously reported results that demonstrated the limitation of the prostatic sextant as a unit of analysis (27,28). Some of this inaccuracy is likely attributable to errors in registration between imaging sections and biopsy specimens. Because of radiation-induced shrinkage and distortion of prostatic tissue, sextant localization is further impaired at both transrectal US and MR imaging, and such errors are likely to be even greater. The presence or absence of recurrent cancer in each prostate side at transrectal US-guided sextant biopsy was used as the standard of reference. A staff pathologist at our institution completed a histopathologic report for all cases, and these reports were reviewed by one of the authors (A.C.W., 5 years of experience in genitourinary imaging). Histopathologic evidence of only a posttreatment effect was considered a negative result (29).

Student t, χ^2, and Mann-Whitney tests were used to compare the distribution of variables between the patients with positive and those with negative biopsy outcomes (Table 1). We used logistic regression with either a single predictor—that is, T2-weighted MR imaging results—or two predictors—specifically, T2-weighted MR imaging results and MR spectroscopic imaging results—to model the probability of a positive outcome. To take into account the clustering effect related to the artificial division of the prostate (right and left sides), we used generalized estimating equations. The performance of each technique was described by using receiver operating characteristic curves. We used cluster resampled bias-corrected bootstrap confidence intervals to compare differences between the areas under the receiver operating characteristic curves (A_Z) (30). Because the use of androgen deprivation therapy may affect the detection of recurrent disease on T2-weighted MR images and MR spectroscopic images differently, we performed a subgroup analysis of the diagnostic performance of these modalities in patients who received and patients who did not receive additional treatment. For all statistical analyses, $P < .05$ was considered to indicate a significant outcome. Statistical calculations were performed by using Stata 11 software (Stata, College Station, Tex).

Results

Clinical Results

The overall median pretreatment PSA level and Gleason score sum at the time of the prostate cancer diagnosis were 9.25 ng/mL (range, 3.50–81.7 ng/mL) and 7 (range, 5–10), respectively. Thirty-three patients received androgen deprivation therapy; data were not available for one patient. Other clinical and treatment characteristics of our patient population are provided in Table 1. The median PSA level at the time of imaging was 2.6 ng/mL (range, 0.7–23.3 ng/mL). Recurrent prostate cancer was identified at biopsy in 37 (58%) of the 64 men and was unilateral in 28 men and bilateral in nine (for total of 46 affected prostate sides). The mean time interval between biopsy and MR imaging was 60 days (range, 0–175 days); the interval for 48 (75%) of the 64 patients was 80 days or less.

Imaging Results

There was a significant difference (P = .001) between A_z values for T2-weighted MR imaging alone (0.67; 95% CI: 0.60, 0.75) and those for the integrated approach involving both T2-weighted MR imaging and MR spectroscopic imaging (0.79; 95% CI: 0.72, 0.86) (Fig 2). The 2 × 2 tables for each approach show that the combined approach involving MR spectroscopic imaging had more true-positive results than did T2-weighted MR imaging alone (59% vs 41%, respectively), without an important change in the number of false-positive results (10% [eight of 82] vs 7% [six of 82], respectively) (Tables 2 and 3). Fourteen prostate sides were incorrectly classified as negative for cancer with both T2-weighted MR imaging and MR spectroscopic imaging, and the diagnosis of recurrent disease was missed in eight patients with the combined approach. The results of both modalities based on biopsy results are summarized in Table 4.

The results of secondary analyses to compare the modalities in the subgroups of patients who did and did not undergo additional treatment with androgen deprivation therapy showed that the A_Z values for T2-weighted MR imaging alone (P = .02) and for combined T2-weighted MR imaging and MR spectroscopic imaging (P = .03) were significantly different. In the patients who received prior androgen deprivation therapy, the A_Z values were 0.69 (95% CI: 0.58, 0.81) and 0.83 (95% CI: 0.72, 0.93), respectively. In the patients who did not receive androgen deprivation therapy, the A_Z values were 0.65 (95% CI: 0.54, 0.75) and 0.76 (95% CI: 0.64, 0.88), respectively.

Table 1

Patients' Diagnostic and Treatment Characteristics

Characteristic	Negative Biopsy	Positive Biopsy	*P* Value*
Age (y)†	69 (52–80)	67 (53–81)	.48‡
Baseline PSA level (ng/mL)§	10.07 (3.50–93.00)	9.25 (3.50–81.70)	.91‖
PSA level (ng/mL)#			.80
<10	13	18	
10–20	7	12	
>20	6	5	
Unknown	1	2	
Gleason score sum#**			.29
≤5	1	4	
6–7	22	25	
≥8	3	8	
Unknown	1	0	
Clinical stage#††			
T1c–T2b	15	21	.28
T2c	3	2	
T3a	6	9	
T3b	2	0	
Unknown	1	5	
Radiation dose (Gy)‡‡	76 (72–82)	72 (65–81)	.03‖
Androgen deprivation therapy§§			
None	10	20	.35
Neoadjuvant	4	5	
Neo plus adjuvant	12	11	
Delayed	1	0	

* Unless otherwise noted, *P* values were calculated at χ^2 testing.

† Mean ages at the time of imaging, with age ranges in parentheses.

‡ Student *t* test.

§ Median baseline PSA level measured at the time of the initial diagnosis, with ranges in parentheses.

‖ Mann-Whitney test.

Data are numbers of patients ($n = 64$).

** Determined at the time of the initial diagnosis.

†† Clinical stage based on 2002 American Joint Committee on Cancer criteria, determined at the time of the initial diagnosis.

‡‡ Median radiation doses, with ranges in parentheses.

§§ Data are numbers of patients ($n = 63$); the androgen deprivation therapy status of one patient was not available.

Table 2

T2-weighted MR Imaging versus Biopsy Results

	Biopsy Result		
MR Imaging Result	Positive	Negative	Total
Positive	19	6	25
Negative	27	76	103
Total	46	82	128

Note.—Data are numbers of results.

Figure 2

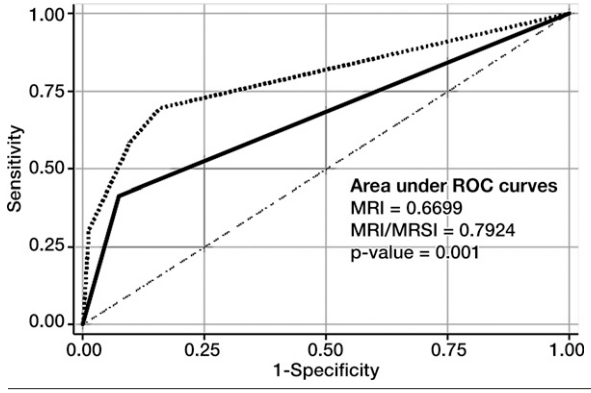

Figure 2: Receiver operating characteristic curves for detection of locally recurrent prostate cancer after external beam radiation therapy (with or without androgen deprivation therapy) with T2-weighted MR imaging (solid line) and combined T2-weighted MR imaging and MR spectroscopic imaging *(MRI/MRSI)* (dotted line). Lower dashed line is reference line.

Discussion

Early diagnosis of recurrent prostate cancer after external beam radiation therapy is important because it may affect patients' outcomes (31). The results of our study suggest that MR imaging is an acceptable noninvasive method to evaluate these patients, but the imaging protocol should include at least MR spectroscopic imaging. Our results also suggest that the benefit of adding MR spectroscopic imaging is not dependent on the androgen deprivation therapy status. To our knowledge, researchers in only two prior studies, involving a population of 30 patients, have investigated the value of using MR spectroscopic imaging to detect recurrent prostate cancer after external beam radiation therapy (15,16). Our study results add to the pool of available data. In addition, in these two studies, the investigators compared the accuracies of T2-weighted MR imaging and MR spectroscopic imaging but did not assess the value of combining the two approaches.

Our results are concordant with prior studies in which the results showed that T2-weighted MR imaging is a poor technique for detecting local recurrence after radiation therapy, mainly because the glands become atrophic and have diffuse low signal intensity. The data suggest that T2-weighted MR imaging has low sensitivity and high specificity when it is used alone and that MR spectroscopic imaging is more sensitive for the detection of recurrent disease than is T2-weighted MR imaging (15–18). Yet, recurrent cancer was missed in eight (22%) of the 37 men with positive

Table 3

MR Spectroscopic Imaging versus Biopsy Results

MR Spectroscopic Imaging Result	Biopsy Result		
	Positive	Negative	Total
Positive	27	8	35
Negative	19	74	93
Total	46	82	128

Note.—Data are numbers of results.

Table 4

Agreement between T2-weighted MR Imaging and MR Spectroscopic Imaging per Biopsy-Side Result

MR Spectroscopic Imaging Result	Negative Biopsy Result Group*			Positive Biopsy Result Group†		
	Positive MR Imaging Result	Negative MR Imaging Result	Total	Positive MR Imaging Result	Negative MR Imaging Result	Total
Positive	1	7	8	14	13	27
Negative	5	69	74	5	14	19
Total	6	76	82	19	27	46

Note.—Data are numbers of results.

* $P = .55$ (cluster-adjusted χ^2 test).

† $P = .08$ (cluster-adjusted χ^2 test).

biopsy results in our study, even when the combined approach was used. That is, the number of false-negative cases was high, and relying only on either of these techniques alone or on both techniques combined could lead to a delay in diagnosis and treatment. It is important to note that MR spectroscopic imaging is not the only additional MR imaging technique that can be used to examine patients suspected of having local recurrence. Other authors have investigated the use of dynamic contrast material–enhanced MR imaging and diffusion-weighted MR imaging in the same clinical scenario (32–34), and their results also showed better accuracy with the combined protocols than with T2-weighted MR imaging alone. Kim et al, for instance, found that the addition of dynamic contrast-enhanced 3-T MR imaging, as compared with T2-weighted MR imaging alone, led to an improvement in the A_Z, from 0.61 to 0.88 (34); these results suggest that this technique may be more accurate than MR spectroscopic imaging for the detection of local tumor recurrence after radiation therapy. Overall, however, the results of the current and prior studies suggest that an approach in which all MR techniques (T2-weighted MR, MR spectroscopic, dynamic contrast-enhanced MR, and diffusion-weighted MR imaging) are incorporated, commonly known as multiparametric MR imaging, could improve the detection of recurrent cancer to more clinically relevant levels. Additional research is needed to confirm this hypothesis.

In 2006, the American Society for Therapeutic Radiology and Oncology (ASTRO) developed and recommended the use of a new definition of biochemical failure after external beam radiation therapy with or without androgen deprivation hormonal therapy. Biochemical failure was defined as an increase in PSA level of 2 ng/mL or more above the nadir level. Validation studies involving use of the Phoenix definition of biochemical failure suggest that it may be a better predictor of local recurrence than the 1996 ASTRO definition (12,35,36). Because biochemical failure is the usual indicator that imaging is needed, new studies are needed to determine if the results obtained in our study persist in patients who are selected on the basis of the new definition.

Our study had limitations. This was a retrospective single-institution study; therefore, our results may not be generalizable, as imaging acquisitions and interpretation expertise vary across institutions, particularly with MR spectroscopy. Our study design did not require a second reader for either the T2-weighted MR or MR spectroscopic images; therefore, we could not assess interreader variability. In addition, a retrospective research design is prone to sample selection bias. We included only those patients who had undergone transrectal US-guided biopsy, and this probably resulted in a greater than expected prevalence of recurrent cancer in our population than in the general population of patients who are treated with external beam radiation therapy. We used biopsy results as the surrogate marker for local tumor recurrence; however, a better standard of reference probably would be salvage prostatectomy specimen findings. Because of possible sampling errors, the use of biopsy as a standard of reference could lead to biased estimations of the accuracy of the imaging examination (37). Salvage prostatectomy, however, is seldom performed. A retrospective design can also introduce verification bias because the decision to perform surgery probably would be influenced by the positive results of imaging. Although our option to use prostate side as the unit of analysis may seem unconventional, it is based on existing data showing the limitations of using sextants to localize disease (27,28). In addition, a recent study by Kumbhani et al revealed that there is no significant difference between the accuracy of MR imaging in the detection of recurrent cancer when the analysis is performed by using sextants and the accuracy when the analysis is performed by using prostate sides (38).

In conclusion, the addition of MR spectroscopic imaging to T2-weighted MR imaging significantly improves the detection of locally recurrent prostate cancer after definitive external beam radiation therapy. The resulting information may assist the clinician in advising patients about subsequent clinical evaluation and selecting those patients for whom targeted prostate-side biopsy is appropriate for confirming disease. Although targeted therapies may be offered to patients in whom very minimal recurrent disease is diagnosed, prostate-side imaging evaluation is sufficiently accurate to obviate sextant

localization because the most commonly recommended salvage therapies (radical retropubic prostatectomy, permanent low-dose-rate brachytherapy) are used to treat the entire gland.

References

1. American Cancer Society. Cancer facts and figures 2009. Atlanta, Ga: American Cancer Society, 2009.
2. Cooperberg MR, Grossfeld GD, Lubeck DP, Carroll PR. National practice patterns and time trends in androgen ablation for localized prostate cancer. J Natl Cancer Inst 2003;95(13):981–989.
3. Stanford JL, Stephenson RA, Coyle LM, et al. Prostate cancer trends 1973-1995: SEER Program, National Cancer Institute. Bethesda, Md: National Cancer Institute, 1999.
4. Vulto JC, Lybeert ML, Louwman MW, Poortmans PM, Coebergh JW. Population-based study of trends and variations in radiotherapy as part of primary treatment of cancer in the southern Netherlands between 1988 and 2006, with an emphasis on breast and rectal cancer. Int J Radiat Oncol Biol Phys 2009;74(2):464–471.
5. Zietman AL, DeSilvio ML, Slater JD, et al. Comparison of conventional-dose vs high-dose conformal radiation therapy in clinically localized adenocarcinoma of the prostate: a randomized controlled trial. JAMA 2005;294(10):1233–1239.
6. Pollack A, Zagars GK, Starkschall G, et al. Prostate cancer radiation dose response: results of the M. D. Anderson phase III randomized trial. Int J Radiat Oncol Biol Phys 2002;53(5):1097–1105.
7. Kestin LL, Vicini FA, Ziaja EL, Stromberg JS, Frazier RC, Martinez AA. Defining biochemical cure for prostate carcinoma patients treated with external beam radiation therapy. Cancer 1999;86(8):1557–1566.
8. McKenna DA, Coakley FV, Westphalen AC, et al. Prostate cancer: role of pretreatment MR in predicting outcome after external-beam radiation therapy—initial experience. Radiology 2008;247(1):141–146.
9. Zelefsky MJ, Fuks Z, Hunt M, et al. High dose radiation delivered by intensity modulated conformal radiotherapy improves the outcome of localized prostate cancer. J Urol 2001;166(3):876–881.
10. Stephenson AJ, Eastham JA. Role of salvage radical prostatectomy for recurrent prostate cancer after radiation therapy. J Clin Oncol 2005;23(32):8198–8203.
11. Jabbari S, Weinberg VK, Shinohara K, et al. Equivalent biochemical control and improved prostate-specific antigen nadir after permanent prostate seed implant brachytherapy versus high-dose three-dimensional conformal radiotherapy and high-dose conformal proton beam radiotherapy boost. Int J Radiat Oncol Biol Phys 2010;76(1):36–42.
12. Abramowitz MC, Li T, Buyyounouski MK, et al. The Phoenix definition of biochemical failure predicts for overall survival in patients with prostate cancer. Cancer 2008;112(1):55–60.
13. Horwitz EM, Bae K, Hanks GE, et al. Ten-year follow-up of radiation therapy oncology group protocol 92-02: a phase III trial of the duration of elective androgen deprivation in locally advanced prostate cancer. J Clin Oncol 2008;26(15):2497–2504.
14. Kuban DA, Thames HD, Levy LB, et al. Long-term multi-institutional analysis of stage T1-T2 prostate cancer treated with radiotherapy in the PSA era. Int J Radiat Oncol Biol Phys 2003;57(4):915–928.
15. Coakley FV, Teh HS, Qayyum A, et al. Endorectal MR imaging and MR spectroscopic imaging for locally recurrent prostate cancer after external beam radiation therapy: preliminary experience. Radiology 2004;233(2):441–448.
16. Pucar D, Shukla–Dave A, Hricak H, et al. Prostate cancer: correlation of MR imaging and MR spectroscopy with pathologic findings after radiation therapy—initial experience. Radiology 2005;236(2):545–553.
17. Sala E, Eberhardt SC, Akin O, et al. Endorectal MR imaging before salvage prostatectomy: tumor localization and staging. Radiology 2006;238(1):176–183.
18. Westphalen AC, Kurhanewicz J, Cunha RM, et al. T2-weighted endorectal magnetic resonance imaging of prostate cancer after external beam radiation therapy. Int Braz J Urol 2009;35(2):171–180; discussion 181–182.
19. Pickett B, Ten Haken RK, Kurhanewicz J, et al. Time to metabolic atrophy after permanent prostate seed implantation based on magnetic resonance spectroscopic imaging. Int J Radiat Oncol Biol Phys 2004;59(3):665–673.
20. American Society for Therapeutic Radiology and Oncology Consensus Panel. Consensus statement: guidelines for PSA following radiation therapy. Int J Radiat Oncol Biol Phys 1997;37(5):1035–1041.
21. Star-Lack J, Vigneron DB, Pauly J, Kurhanewicz J, Nelson SJ. Improved solvent suppression and increased spatial excitation bandwidths for three-dimensional PRESS CSI using phase-compensating spectral/spatial spin-echo pulses. J Magn Reson Imaging 1997;7(4):745–757.
22. Schricker AA, Pauly JM, Kurhanewicz J, Swanson MG, Vigneron DB. Dualband spectral-spatial RF pulses for prostate MR spectroscopic imaging. Magn Reson Med 2001;46(6):1079–1087.
23. Tran TK, Vigneron DB, Sailasuta N, et al. Very selective suppression pulses for clinical MRSI studies of brain and prostate cancer. Magn Reson Med 2000;43(1):23–33.
24. Rajesh A, Coakley FV. MR imaging and MR spectroscopic imaging of prostate cancer. Magn Reson Imaging Clin N Am 2004;12(3):557–579, vii.
25. Fayad LM, Salibi N, Wang X, et al. Quantification of muscle choline concentrations by proton MR spectroscopy at 3 T: technical feasibility. AJR Am J Roentgenol 2010;194(1):W73–W79.
26. Kurhanewicz J, Swanson MG, Nelson SJ, Vigneron DB. Combined magnetic resonance imaging and spectroscopic imaging approach to molecular imaging of prostate cancer. J Magn Reson Imaging 2002;16(4):451–463.
27. Wefer AE, Hricak H, Vigneron DB, et al. Sextant localization of prostate cancer: comparison of sextant biopsy, magnetic resonance imaging and magnetic resonance spectroscopic imaging with step section histology. J Urol 2000;164(2):400–404.
28. Obek C, Louis P, Civantos F, Soloway MS. Comparison of digital rectal examination and biopsy results with the radical prostatectomy specimen. J Urol 1999;161(2):494–498; discussion 498–499.
29. Kestin LL, Goldstein NS, Vicini FA, et al. Pathologic evidence of dose-response and dose-volume relationships for prostate cancer treated with combined external beam radiotherapy and high-dose-rate brachytherapy. Int J Radiat Oncol Biol Phys 2002;54(1):107–118.
30. Davison A, Hinkley D. Bootstrap methods and their application. Cambridge, England: Cambridge University Press, 1997.
31. Pollack A, Zagars GK, Antolak JA, Kuban DA, Rosen II. Prostate biopsy status and PSA nadir level as early surrogates for treatment failure: analysis of a prostate cancer randomized radiation dose escalation trial. Int J Radiat Oncol Biol Phys 2002;54(3):677–685.
32. Haider MA, Chung P, Sweet J, et al. Dynamic contrast-enhanced magnetic resonance imaging for localization of recurrent prostate

cancer after external beam radiotherapy. Int J Radiat Oncol Biol Phys 2008;70(2):425–430.

33. Rouvière O, Valette O, Grivolat S, et al. Recurrent prostate cancer after external beam radiotherapy: value of contrast-enhanced dynamic MRI in localizing intraprostatic tumor—correlation with biopsy findings. Urology 2004;63(5):922–927.
34. Kim CK, Park BK, Lee HM. Prediction of locally recurrent prostate cancer after radiation therapy: incremental value of 3T diffusion-weighted MRI. J Magn Reson Imaging 2009;29(2):391–397.
35. Morgan PB, Hanlon AL, Horwitz EM, Buyyounouski MK, Uzzo RG, Pollack A. Timing of biochemical failure and distant metastatic disease for low-, intermediate-, and high-risk prostate cancer after radiotherapy. Cancer 2007;110(1):68–80.
36. Ramalingam M, Lau W, Tan T, Fook S, Ngoi F, Cheng C. Asians with localized prostate cancer treated with 3-dimensional conformal radiation therapy and adjuvant hormonal therapy: comparing Phoenix and American Society of Therapeutic Radiology and Oncology (ASTRO) definitions in an Asian population. Urology 2008;71(3):506–510.
37. Hawkins DM, Garrett JA, Stephenson B. Some issues in resolution of diagnostic tests using an imperfect gold standard. Stat Med 2001;20(13):1987–2001.
38. Kumbhani SR, Kurhanewicz J, Coakley FV, Weinberg VK, Qayyum A, Westphalen AC. Endorectal T2-weighted MR imaging for the detection of recurrent prostate cancer after external beam radiation therapy: accuracy of different interpretative approaches (abstr). In: Radiological Society of North America scientific assembly and annual meeting program. Oak Brook, Ill: Radiological Society of North America, 2009; 873.